# Effect of nitrogen interactions on photoluminescence linewidth broadening in dilute nitride semiconductors

I. Bosa,[1] D. McPeake,[1] and S. Fahy[2]
[1]*Tyndall National Institute, Lee Maltings, Prospect Row, Cork, Ireland*
[2]*Department of Physics and Tyndall National Institute, University College Cork, Cork, Ireland*
(Received 29 October 2008; published 23 December 2008)

A random potential model of inhomogeneous photoluminescence (PL) linewidth broadening at low temperature in the dilute nitride semiconductor alloy GaAsN is presented, with model parameters determined from *n*-type carrier mobility and effective mass only. The low-temperature line shapes obtained by numerical solution of this model are consistent with those seen in existing near-field scanning optical microscopy (NSOM) and conventional PL spectra. The size of low-lying localized states obtained in the model is consistent with observed diamagnetic shifts of sharp spectral features of the NSOM spectra. The overall width of the PL spectrum is found to be substantially increased by N-N interactions in carrier scattering processes, corresponding to strong reductions in carrier mobility due to such interactions, but is consistent with a random distribution of substitutional nitrogen in the alloy. Comparison with the sharp emission line features of NSOM spectra allows us to estimate the exciton capture regions in these materials at low temperature to be of the order of 50 nm in size.

DOI: 10.1103/PhysRevB.78.245206 PACS number(s): 78.55.Cr, 78.20.Bh, 61.43.−j, 68.37.Uv

## I. INTRODUCTION

The unusual electronic properties exhibited by the ternary and quaternary dilute nitride alloys, Ga(In)AsN, have been the subject of a major research effort in recent years. Incorporation of a small concentration of nitrogen into GaAs alloys (principally by substitution on the group-V sites) dramatically decreases the band-gap energy (1% of nitrogen reducing the gap by approximately 150 meV). Adding 3% of N brings the band gap close to 1 eV, which makes these materials very attractive candidates for long-wavelength laser applications in telecommunications[1–3] and for high-efficiency multijunction solar cells.[3,4]

However, this addition of a small amount of nitrogen into GaAs is accompanied by a marked deterioration of the optical and transport properties of the material: inhomogeneous linewidth broadening of the photoluminescence (PL) spectra,[5–8] substantial decrease in *n*-type carrier mobility[9–13] and lifetime,[11] and increase in carrier effective mass.[14] These observations are considered to be evidence of strong disorder in the materials, which has been attributed in part to spatial fluctuations of nitrogen composition[8,15–17] and to resonant interaction of nitrogen-induced quasilocalized states with the conduction band.[18–20] The structural characterization of these fluctuations is the subject of further theoretical and experimental researches.[16,17,21–25]

In this paper, we point out a fundamental general connection between carrier mobility and PL linewidth in random alloys, where the disorder and carrier mobility are dominated by short-range potential fluctuations and elastic scattering. We use the experimentally determined *n*-type carrier mobility and effective mass in the dilute nitrides to estimate the strength of the random spatial fluctuations of the effective potential for electrons near the conduction-band edge and we explore the consequences for PL linewidth by numerically calculating the states of the associated random potential model. In relation to the effects of random nitrogen incorporation in GaAs, it has been shown[20] that N-N interactions in the alloy give rise to much lower carrier mobility (and correspondingly larger effective potential fluctuations) than would be expected if N-N interactions were neglected; this applies for a completely random distribution of N on the group-V sites. These large effective potential variations give rise to strong localization of excitons and a large inhomogeneous PL linewidth, without any appeal to preferential nitrogen clustering or partial phase segregation in the material.[8,15]

Variations in the N concentration in different spatial regions of GaAsN alloy lead to fluctuations in the local band-gap energy. Based on the assumption that each alloy site scatters electrons independently (i.e., neglecting multiple scattering or multiple-site interactions), Shlimak *et al.*[26] (considering SiGe alloys) and Fahy and O'Reilly[27] (considering the dilute nitrides) showed that the carrier mobility $\mu$ is proportional to $(dE/dx)^{-2}$, where $E(x)$ is the energy of the alloy band edge at composition $x$. (As we shall see later in this paper, the assumption of independent scattering by each N site is equivalent to the assumption that the shift in the local band edge is proportional to the local N concentration.) Although the results demonstrate qualitatively the intimate connection between poor carrier mobility and rapid variation in the band gap with alloy composition, the mobility calculated for *n*-type carriers in GaAsN (Ref. 27) under these assumptions is still substantially higher than the measured values.

Fluctuations of the local band edge also give rise to strong inhomogeneous broadening of PL spectra.[28–32] Mintairov *et al.*[7,15] analyzed PL spectra of dilute nitrides from near-field scanning optical microscopy (NSOM) measurements in terms of a model, in which the change in the local band edge is determined by the local nitrogen concentration within the exciton volume. In this model, the local band-edge shift is assumed to be $\Delta E=(dE/dx)\Delta x$, where $\Delta x$ is the local nitrogen concentration. Using this analysis and associating sharp lines observed in the PL spectrum with distinct quantum

 

dots, Mintairov *et al.*[7,15] found that the N concentration variations implied were inconsistent with a random distribution. For a region of the size of the exciton (~10 nm across) at 3% of N, the band-edge fluctuations estimated from this model[28] are about 8 meV. It was concluded that the linewidth and structure of the PL spectra indicate phase separation in the distribution of the nitrogen in the material, i.e., spontaneous formation of nonrandom nitrogen clusters.

Neither the analysis of mobility in Ref. 27 nor the model of band-edge fluctuations used to estimate the PL linewidth in Refs. 7, 15, and 28–30 taking into account interactions between N sites. However, Lindsay and O'Reilly[18,19] showed that these interactions have a very important influence on the states near the conduction-band edge in the dilute nitrides. Such interactions occur, even when nitrogen is randomly distributed in the alloy. Fahy *et al.*[20] showed that the N-N interactions give rise to a large increase in the carrier scattering and a corresponding reduction in mobility in dilute nitrides. Their results show good agreement with the observed experimental values for band-gap bowing,[18,19] carrier mobility,[20] and carrier effective mass.[14]

## II. GENERAL RELATION BETWEEN POTENTIAL FLUCTUATIONS AND ALLOY SCATTERING

In this paper we re-examine the carrier mobility and PL broadening in terms of a model which assumes random spatial variations in the band edge but does *not* assume that these fluctuations arise solely from variations in the nitrogen concentration. (When interactions between nitrogen atoms are taken into account, not only the local nitrogen concentration but also the specific arrangement of the atoms in a locality has a large effect on the band edge.[18,19]) We assume only that band gaps in different regions $dR$ and $dR'$, each substantially larger than the cubic lattice constant but smaller than de Broglie wavelength of the carriers, are statistically independent. We use the experimentally observed $n$-type carrier mobility and effective mass to estimate the strength of fluctuations of the potential in different regions of the solid.

To derive the relation between the carrier mobility and the local energy fluctuations, we begin with the elastic-scattering cross section between two carrier states,[33] $\phi_k$ and $\phi_{k'}$ of momentum $k$ and $k'$, respectively. The scattering matrix element in the presence of a localized perturbing potential $\Delta V$ is $\langle\psi_k|\Delta V|\phi_{k'}\rangle$, where $\psi_k$ is the exact eigenstate in the presence of the perturbation.[33] [We assume $\psi_k(\mathbf{r}) \sim \phi_k(\mathbf{r})$ at points $\mathbf{r}$ very far from the perturbation.] For low-energy scattering, both $k$ and $k'$ are approximately zero and for a sufficiently localized perturbation (i.e., where the range of $\Delta V$ is less than $2\pi/|\mathbf{k}-\mathbf{k}'|$) the scattering matrix element is approximately independent of $k$ and $k'$.[27] The total scattering cross section for this localized perturbation is then given by:[27]

$$\sigma(R) = 4\pi\left(\frac{m^*}{2\pi\hbar^2}\right)^2 |\langle\psi_0|\Delta V|\phi_0\rangle|^2\Omega^2, \tag{1}$$

where $m^*$ is the carrier effective mass and $\Omega$ is the volume in which the states $\phi_0$ and $\psi_0$ are normalized.

If $\Delta V(R)$ is the change in potential in a small region of volume $dR$ centered at $R$, compared to the average potential across the entire system, the scattering matrix element due to that potential fluctuation can then be rewritten as

$$\langle\psi_0|\Delta V(R)|\phi_0\rangle\Omega = \delta E_{dR}(R)dR, \tag{2}$$

where $\delta E_{dR}dR/\Omega$ is the change in the energy of the state due to the perturbation $\Delta V(R)$ and $\delta E_{dR}$ is the equivalent shift of the average band gap in the region $dR$.

Dividing all space into small nonoverlapping volume elements and considering each element $dR$ as a scattering center, statistically independent of other elements, the density of these scatterers is $n=1/dR$ and the inverse of the carrier mean-free path is given by

$$\frac{1}{l} = n\langle\sigma(R)\rangle = \langle\sigma(R)\rangle/dR, \tag{3}$$

where the angular brackets indicate an ensemble average over the random alloy. The carrier mobility $\mu$ is related to the mean-free path as $\mu=el/\bar{u}m^*$, where $\bar{u}$ is the mean carrier velocity. Setting $\bar{u}=\sqrt{3k_BT/m^*}$, where $T$ is the absolute temperature, we obtain the following relation between the mobility $\mu$ and the band-gap fluctuations $\delta E_{dR}$:

$$\mu^{-1} = \frac{\sqrt{3m^*k_BT}}{e}\pi\left(\frac{m^*}{\pi\hbar^2}\right)^2 dR\langle\delta E_{dR}^2\rangle. \tag{4}$$

Note that when the region $dR$ is itself composed of many statistically independent subregions, each contributing independently to the average band gap $\delta E_{dR}$ in the region $dR$, we have that $dR\langle\delta E_{dR}^2\rangle$ is well defined and independent of the size of the volume element $dR$. Recall also that, in using Eq. (1) for the scattering cross section of the region $dR$, we assume that $dR$ is smaller than the de Broglie wavelength of the carriers. Thus, Eq. (4) is valid when the typical de Broglie wavelength of the carriers is larger than the correlation length of the spatial variations in the band gap.

In the ultradilute case, when each nitrogen atom can be considered as an independent scattering center, each nitrogen contributes $dE_c/dn$ to the left-hand side of Eq. (2),[27] where $E_c$ is the conduction-band energy and $n$ is the average number of nitrogen atoms per unit volume. In the region $dR$, where we have $N_{dR}(R)$ nitrogen atoms, the total contribution is $(dE_c/dn)N_{dR}(R)$ and for $\langle\delta E_{dR}^2\rangle$ we can write

$$\langle\delta E_{dR}^2\rangle = \left|\frac{dE_c}{dn}\right|^2\frac{\langle[N_{dR}(R)-ndR]^2\rangle}{dR^2}. \tag{5}$$

For a dilute random alloy $N_{dR}(R)$ is a Poisson random variable with variance $\langle[N_{dR}(R)-ndR]^2\rangle=ndR$. Noting that $n$ is related to the nitrogen atomic concentration $x$ on the group-V sites as $n=4x/a_0^3$, we replace the term $dR\langle\delta E_{dR}^2\rangle$ in Eq. (4) with

$$dR\langle\delta E_{dR}^2\rangle = \left|\frac{dE_c}{dn}\right|^2 n = \left|\frac{dE_c}{dx}\right|^2\frac{a_0^3}{4}x, \tag{6}$$

thus recovering the result for the mobility given in Eq. (7) of Ref. 27.

In a nondilute random binary alloy of average concentration $x$, $N_{dR}(R)$ has a binomial distribution with variance $\langle[N_{dR}(R)-ndR]^2\rangle=x(1-x)dN_s$, where $dN_s$ is the number of

sites in the region $dR$. Assuming that each site scatters independently, we then have that

$$dR\langle \delta E_{dR}^2 \rangle = \left| \frac{dE_c}{dx} \right|^2 V_s x(1-x), \tag{7}$$

where $V_s$ is the volume per site in the alloy, and obtain the following form[26] for the mobility:

$$\mu^{-1} = \frac{\sqrt{3m^* k_B T}}{e} \pi \left( \frac{m^*}{\pi \hbar^2} \right)^2 \left| \frac{dE_c}{dx} \right|^2 V_s x(1-x). \tag{8}$$

To go beyond the approximation of independent scattering by the N sites, which is clearly invalid in the dilute nitride alloys, we use the measured mobility and Eq. (4) to phenomenologically define the strength of the fluctuations $\langle \delta E_{dR}^2 \rangle$ in the band gap in regions of volume $dR$. This does not impose any assumption on the microscopic origin of the disorder that causes the band-gap variations—only as mentioned above that the correlation length of the variations is less than the de Broglie wavelength of the carriers. Note that the only parameters determining the strength of the disorder from Eq. (4) are the carrier mobility and effective mass in the material. Because our analysis of carrier scattering and mobility assumes that the current is carried by delocalized states, rather than by hopping between localized states, it is preferable to use room-temperature mobility (rather than low-temperature mobility) to estimate the fluctuations in the random potential. The measured mobility of electrons in GaAsN alloys with 3% of N is $\sim 150$ cm$^2$/V s at room temperature, giving a calculated local energy variation $\langle \delta E_{dR}^2 \rangle$ from Eq. (4) of $\sim 25$ meV when $dR$=one exciton volume (sphere with radius 5 nm) and the effective mass is $0.13m_e$ ($m_e$ is mass of the electron).[18]

We note that for regions smaller than the exciton volume, the band-gap variation will be even larger. This variation is much greater than the electron-hole binding energy ($\sim 4.2$ meV for GaAs). Therefore the random potential will dominate over the electron-hole attraction in these strongly disordered alloys and the electron-hole Coulomb interaction can be neglected. The size of potential variations also indicates that first-order perturbation[28–30] is no longer sufficient to obtain the PL linewidth since the wave function is strongly distorted by the potential $\Delta V$ and higher orders of perturbation (or direct numerical calculation) have to be used to find the exciton energies. Strong disorder arising from the large band-gap variations also causes localization of the low-energy exciton states and they become trapped in the local minima of the potential. This implies that, particularly at low temperature, PL will come predominantly from excitons trapped in the regions of lowest band gap.[34]

## III. CALCULATION OF STATES FOR THE RANDOM POTENTIAL MODEL

To calculate the electron energy states in the disordered alloy, we use the effective-mass approximation, so that the conduction-band electrons are assumed to be particles of mass $m^*$ in a random potential $V_{\text{rand}}$ and the Schrödinger equation has the form[35–37]

$$\left[ -\frac{\hbar^2}{2m^*} \nabla^2 + V_{\text{rand}}(\mathbf{r}) \right] \chi(\mathbf{r}) = (E - E_c)\chi(\mathbf{r}). \tag{9}$$

The energy of the electrons is measured from the bottom of the conduction band $E_c$ and $\chi(\mathbf{r})$ is the electron envelope wave function in the effective-mass approximation. We assume that the random potential has a Gaussian distribution as follows:

$$\langle V_{\text{rand}}(\mathbf{r}) \rangle = 0, \tag{10}$$

$$\langle V_{\text{rand}}(\mathbf{r}) V_{\text{rand}}(\mathbf{r}') \rangle = C \frac{e^{[-(\mathbf{r}-\mathbf{r}')^2/L_{\text{corr}}^2]}}{\pi^{3/2} L_{\text{corr}}^3}, \tag{11}$$

where $\mathbf{r}$ is the coordinate of the electron, $L_{\text{corr}}$ is the spatial correlation length of the random potential, which we will discuss further below, and $C$ defines the strength of the random potential variations. This definition of $V_{\text{rand}}$ is consistent with Eq. (4) when

$$\frac{1}{C} = \frac{\sqrt{3m^* k_B T}}{e} \pi \left( \frac{m^*}{\pi \hbar^2} \right)^2 \mu. \tag{12}$$

To solve this model numerically, it is convenient to represent both $\chi$ and $V_{\text{rand}}$ in terms of their Fourier series, assuming periodic boundary conditions on a cube of side $L$. Thus, the potential is of the form

$$V_{\text{rand}}(\mathbf{r}) = \sum_{\mathbf{q}} \tilde{V}(\mathbf{q}) \frac{\exp[i\mathbf{q} \cdot \mathbf{r}]}{L^{3/2}}, \tag{13}$$

where $\mathbf{q}$ is summed over wave vectors compatible with periodic boundary conditions on the cube. The real and imaginary parts, $\Re \tilde{V}(\mathbf{q})$ and $\Im \tilde{V}(\mathbf{q})$, of the Fourier components $\tilde{V}(\mathbf{q})$ are random Gaussian independent variables, with $\langle \tilde{V}(\mathbf{q}) \rangle = 0$, and $\langle |\Re \tilde{V}(\mathbf{q})|^2 \rangle = \langle |\Im \tilde{V}(\mathbf{q})|^2 \rangle = (C/2)\exp[-(qL_{\text{corr}}/2)^2]$ for $\mathbf{q} \neq \mathbf{0}$. Since the potential $V_{\text{rand}}(\mathbf{r})$ is real, it follows that $\tilde{V}(-\mathbf{q}) \equiv \tilde{V}^*(\mathbf{q})$ for all $\mathbf{q}$, and that $\langle |\Re \tilde{V}(\mathbf{q}=\mathbf{0})|^2 \rangle = C$ and $\langle |\Im \tilde{V}(\mathbf{q}=\mathbf{0})|^2 \rangle = \mathbf{0}$. Having chosen by Monte Carlo sampling a particular set of random values for the Fourier components of the potential, we then solve for the energy eigenstates by numerical diagonalization of the resulting Hamiltonian $H_{\mathbf{k},\mathbf{k}'}$ in the momentum representation, where

$$H_{\mathbf{k},\mathbf{k}'} = \frac{\hbar^2 k^2}{2m^*} \delta_{\mathbf{k},\mathbf{k}'} + \frac{\tilde{V}(\mathbf{k}-\mathbf{k}')}{L^{3/2}}. \tag{14}$$

We note that the random potential model is ill conditioned in the limit as $L_{\text{corr}} \to 0$,[35] giving a spectrum of energies unbound below. However, in the context of the dilute nitride alloys, it is clear that $L_{\text{corr}}$ can be no less than the interaction distance between nitrogen defects. Calculations of Lindsay *et al.*[18,19] demonstrated substantial interaction between N atoms up to approximately 1 nm, so that regions of dimension less than 1 nm cannot be considered to be statistically independent scattering centers. Furthermore, the effective-mass model in GaAs assumes that alloy states are predominantly made up of Bloch states near the conduction-band minimum. We estimate that the model is limited at best to wave vectors

of length no greater than 1/10 of the Brillouin-zone radius, where the effective-mass band energy is well below the $L$-point conduction-band edge. This provides a natural cutoff in the wave vectors $\mathbf{k}$ in the Hamiltonian specified in Eq. (14) and Fourier components of the potential with wave vector larger than approximately 1/5 of the Brillouin-zone radius may be excluded from the effective random potential within the effective-mass model. Transforming back from Fourier space to real space, this defines an effective correlation length of approximately 2–3 nm for the random band-gap model specified in Eqs. (9)–(11). We take $L_{\mathrm{corr}}=5a_0$, but changing in this value only causes a minor shift[35] in the PL spectra simulated (below).

We note that this model does not include the binding of excitons to specific defect structures (e.g., related to particular clustered arrangements of nitrogen), with associated well-defined energies. In the real material such binding may in fact occur but is not included within this random potential effective-mass model. Nevertheless, as we will see below, the model predicts highly structured NSOM PL spectra due to the random variations in the spectrum of states occurring in different finite regions of the material.

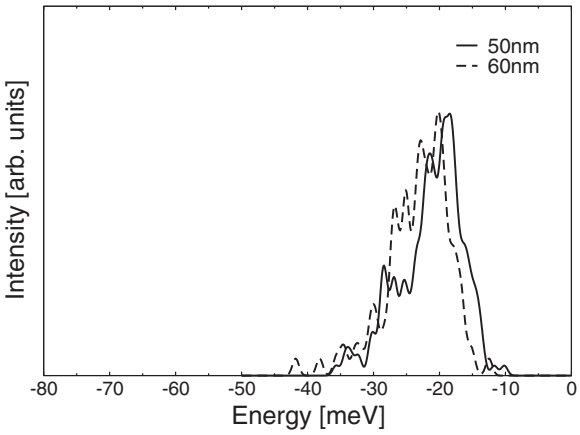


FIG. 1. Simulated low-temperature PL spectra for the random potential model in a volume of 0.025 $\mu\mathrm{m}^3$. The effective mass $m^*=0.13m_e$ and potential fluctuations correspond to a room-temperature mobility $\mu=150\ \mathrm{cm}^2/\mathrm{V\ s}$ in Eqs. (9)–(12), each typical of $GaN_xAs_{1-x}$ with $x\sim 3\%$. The solid line corresponds to the calculation using 200 capture regions, each of volume $(50\ \mathrm{nm})^3$, and the dashed line to the calculation using 116 capture regions, each of volume $(60\ \mathrm{nm})^3$; see text for details.

## IV. SIMULATION OF PHOTOLUMINESCENCE SPECTRA

We now consider the consequences of the random potential-energy spectra for low-temperature PL. Once an electron-hole pair is created, it will rapidly relax its energy by phonon emission (phonon absorption being strongly suppressed at low temperature) and the electron will be trapped in a local minimum of energy, close to the point where it was created, before it eventually recombines with the hole, emitting light which is collected in the PL spectrum.[34] The trapping is preceded by the hopping transport of the exciton, where the electron can hop through the energy states over a limited "capture" region of the solid. (The nitrogen-induced disorder in the valence band is relatively weak and we assume that, due to the electron-hole attraction, the hole follows the electron position.) Thus, in this standard picture of low-temperature PL emission, the PL spectrum from a given NSOM tip region gives the energy distribution of the lowest-energy electron eigenstates in the collection of capture regions covered by the NSOM tip—each capture region contributing one emission line to the overall spectrum.

Without a detailed knowledge of all relaxation processes, it is difficult to calculate the size of the capture region typically explored by the exciton before trapping and recombination. However, we can make sensible lower and upper estimates for the dilute nitrides, which turn out to constrain the size of the capture region within a relatively small range of possible values. First, the capture region must be substantially larger than the size of the typical low-lying localized wave function in the random potential; from direct numerical calculation of the eigenstates in regions of size $L=20-60$ nm, we find that the typical size of low-lying eigenstates of $H$ defined in Eq. (14) is of the order of 10 nm when the effective mass $m^*=0.13m_e$ and the random potential fluctuations correspond to a room-temperature mobility, $\mu=150\ \mathrm{cm}^2/\mathrm{V\ s}$ in Eqs. (9)–(12), which is characteristic of the dilute nitrides at nitrogen concentration of the order of a few percent. (We note that this size also agrees well with values measured experimentally using near-field magneto-photoluminescence.[7] Incidentally, there is no distinction in our numerical calculations between "strongly" and "weakly" localized states—all states, from the most localized to completely delocalized states, are obtained from the numerical calculation. However, the typical size of localized states decreases with decreasing energy, as expected.) Second, since the low-temperature NSOM PL spectra, obtained by Mintairov *et al.*[7,8,15] from NSOM tip regions of the order of a few hundred nanometers across, show many emission energies, it is clear that the tip region contains at least of the order of 100 separate capture regions. Thus, the typical capture region at low temperature must be of the order of several tens of nanometer across.

The simulated low-temperature PL spectra, shown in Fig. 1, are calculated as follows: we assume that the NSOM tip records photoluminescence events occurring in a volume $V_{\mathrm{tip}}=0.025\ \mu\mathrm{m}^3$. This volume is assumed to consist of $N_{\mathrm{cr}}=V_{\mathrm{tip}}/L^3$ capture regions, each is a cube of volume $L^3$. For each capture region, a random potential is constructed using Eq. (13) and the lowest state energy of the resulting Hamiltonian $H_{\mathbf{k},\mathbf{k}'}$, defined in Eq. (14), is taken as the PL emission energy from that capture region. (This emission line is broadened to a Gaussian of width 0.5 meV, corresponding to the experimental energy resolution.[7]) The PL spectrum for the entire region $V_{\mathrm{tip}}$ is then taken as the superposition of the $N_{\mathrm{cr}}$ emission lines from these capture regions. Simulations with capture regions of sizes $L=50$ nm and $L=60$ nm are shown in Fig. 1. We observe very good agreement with the experimental NSOM PL spectra:[7] highly structured PL spectra, with a markedly asymmetric overall line shape of width approximately 15 meV, a relatively sharp cutoff at the high-energy side, and an extended low-energy tail.

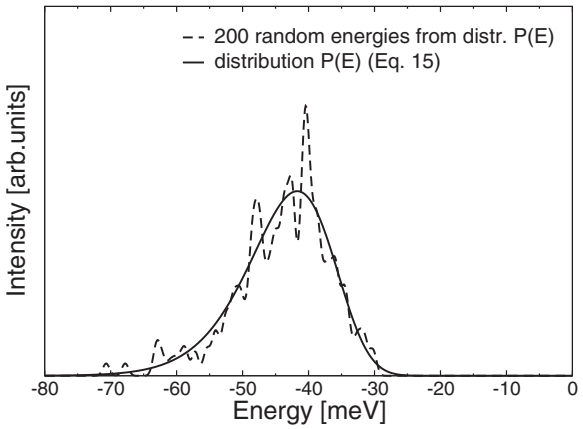


FIG. 2. Spectrum of 200 randomly chosen energies from the distribution $P(E)$ in Eq. (15), with $N_{ex}=125$ and $\sigma=17$ meV, corresponding to a localized exciton volume of $(10\ \text{nm})^3$ and a capture region with $L=50$ nm. Each sampled energy is broadened to a Gaussian line shape of width 0.5 meV.

## V. DISCUSSION AND CONCLUSIONS

The overall shape of the simulated spectra may be understood qualitatively as follows: within each capture region, the exciton has sufficient time before recombination to seek out the lowest-energy state available. This amounts to finding that place within the capture region which has the lowest average potential. (Since all low-lying states have similar size, the kinetic energy due to confinement is approximately equal for all such states, giving only an overall shift of the state energy which can be ignored for the present discussion.) Consider the capture volume as divided into $N_{ex}$ subvolumes $\Omega_i$, each of size equal to that of a typical low-lying localized exciton, in which the average potential is $\bar{V}_i$. The low-temperature exciton emission energy from the capture region is then $\bar{V}_0$, which is the lowest $\bar{V}_i$ occurring within the capture region. (This neglects the overall shift of the exciton energy due to the kinetic energy of electron confinement.) The distribution of $\bar{V}_i$ is a Gaussian with average zero and variance $\sigma^2=C/\Omega_i$. Thus, the distribution function of $\bar{V}_0$ is that of the lowest of a set of $N_{ex}$ independent Gaussian variables,

$$P(E)=\frac{e^{-(E^2/2\sigma^2)}}{\sqrt{2\pi}\sigma}N_{ex}[1-\text{erf}(E/\sigma)]^{N_{ex}-1}, \qquad (15)$$

where $\text{erf}(z)=\int_{-\infty}^{z}e^{-\xi^2/2}d\xi/\sqrt{2\pi}$. The PL spectrum from an entire sample, with an extremely large number of capture regions, is then proportional to this distribution function $P(E)$. For $N_{ex}=1$, $P(E)$ is simply the original Gaussian distribution of $V_i$. However, as $N_{ex}$ increases, the distribution function moves to lower energies and (for $N_{ex}\gg 10$) acquires an increasingly asymmetric line shape similar to the experimental PL spectra and to the simulated spectra shown in Fig. 1. For example, with $N_{ex}=200$, the maximum of $P(E)$ occurs at $E_{max}\approx -2.6\sigma$ and falls off sharply for $E>E_{max}$. In the low-energy tail, $E<E_{max}, P(E)\approx\frac{N_{ex}}{\sqrt{2\pi}\sigma}\exp[-\frac{E^2}{2\sigma^2}]$. Figure 2 shows the histogram generated with 200 samples from $P(E)$ with $N_{ex}=125$ and $\sigma=17$ meV, corresponding to a localized exciton volume of $(10\ \text{nm})^3$ and a capture region with $L=50$ nm. The histogram with 200 samples is shown to indicate the kind of PL spectral fluctuations expected in an NSOM tip volume of 0.025 $\mu\text{m}^3$, as in Fig. 1. This indicates that the ratio of the low-temperature capture region volume to the localized exciton volume is of the order of 100, in agreement with our earlier estimate of the size of the capture region.

The individual sharp peaks in the simulated PL spectra (Fig. 1) are simply due to random variations in the limited sample of $N_{cr}$ emission energies. (For example, when $N_{cr}$ is increased to 1000, a noticeably smoother spectrum is obtained.) As the overall appearance of the simulated spectrum (in relation to the magnitude of the individual sharp peaks) for $N_{cr}$ in the range of 100–200 (particularly closer to 100) is very similar to that observed experimentally, this would suggest that the peaks observed in the NSOM PL spectra may be just such random fluctuations and that the NSOM tip region includes approximately 100 low-temperature capture regions.

The experimental low-temperature NSOM PL spectra obtained in Refs. 7 and 15 were analyzed as consisting of sharp narrow peaks with half width of 0.5–2 meV superimposed on several broad bands with half width equal 20–60 meV. The narrow peaks were attributed to emission of strongly localized excitons from regions with high concentration of N atoms creating a strong confining potential in the material. The broad bands were attributed to regions of weak localization of excitons in the ternary layers and the half width of the emission spectra was interpreted as the energy scale associated with statistical composition fluctuations in the sampled volume.[7,8,15]

Our calculations show that low-temperature spectra very similar to those observed in the NSOM experiments arise from a purely random model of the band-gap fluctuations, consistent with the typical observed effective mass of carriers $0.13m_e$ and mobility 150 $\text{cm}^2(\text{V s})^{-1}$ in the dilute nitrides and assuming regions of size 50–60 nm, in which the initially excited electron-hole pairs recombine. No assumptions of preferential clustering or partial nitrogen phase segregation are required to reproduce the overall PL line shape or the sharp emission lines observed in NSOM PL spectra. The increase in PL linewidth, compared to a model in which nitrogen concentration variations alone cause local band-edge fluctuations, can be attributed to N-N interactions, which greatly increase carrier scattering, decreasing mobility and increasing band-edge fluctuations.[20]

Within the random potential model presented here, the structure of sharp emission lines in the NSOM PL spectrum is a consequence only of the finite size of the region from which the NSOM tip collects its spectrum. The PL spectrum from a given tip region is a finite histogram sampled from the smooth spectrum that would be observed in conventional PL from a large sample. Decreasing the size of the NSOM tip results in a reduced sample size and increased graininess of the histogram, with correspondingly more pronounced emission lines in the spectrum. In the extreme limit, if the NSOM tip region were to include only a single capture region, the histogram from that region would become a single

sharp emission line. (Of course, by moving the tip to a different region, a different line would be observed.) In a homogeneous random model of the PL emission lines, increasing the size of the NSOM tip increases the size of the statistical sample contributing to the observed PL spectrum and individual sharp emission lines are less pronounced. In the infinite size, conventional macro-PL limit, the spectrum becomes smooth [e.g., as shown corresponding to distribution $P(E)$ in Fig. 2], which is similar to the spectrum observed in macro-PL experiments.[5,6]

On the other hand, if specific well-defined defect structures in the material (such as specific nitrogen cluster arrangements, occurring either purely randomly or preferentially) bind localized excitons and give rise to sharp PL emission lines, such emission lines should be clearly observable in the PL spectrum from a large sample. If long-range nonrandom variations occur in the band gap, these will be most clearly observable as systematic shifts in the overall spectrum (rather than specific sharp lines) in the NSOM PL spectra taken in different regions.

The real dilute nitride materials may have a combination of all these effects: true random variations, defect-bound excitons, and long-range composition variation. Each shows a different characteristic dependence on the NSOM tip size and a careful statistical treatment of the observed spectra is required to distinguish among them. However, by systematically varying the NSOM tip size, one can distinguish clearly between the different contributions to linewidth broadening. As discussed here within the model of a purely random potential, the peak structure of the existing NSOM PL spectra gives important information on the size of the low-temperature recombination regions.

In conclusion, we have presented a simple random potential model of low-temperature PL spectra in the dilute nitrides, with parameters determined from *n*-type carrier mobility and effective mass only and consistent with a random distribution of substitutional nitrogen in the alloy. The low-temperature line shapes obtained from this model are consistent with those seen in existing NSOM and conventional PL spectra. The size of low-lying localized states obtained in the model is consistent with observed diamagnetic shifts of sharp features of the NSOM spectra. The overall width of the spectrum is seen to be substantially increased by N-N interactions in carrier scattering processes, corresponding to strong reductions in carrier mobility due to such interactions. Comparison with the sharp emission line features of NSOM spectra allows us to estimate the exciton capture regions in these materials at low temperature to be of the order of 50 nm in size. The dynamics of the electrons prior to recombination and effects of nonradiative recombination centers are strongly influenced by sample temperature. Simulation of these dynamics and of the temperature dependence of the PL spectra is the subject of ongoing investigation.

## ACKNOWLEDGMENTS

The authors wish to thank E. O'Reilly, A. Lindsay, J. Merz, and A. Mintairov for useful discussions. This work was supported by the Science Foundation Ireland.

[1] H. Riechert, A. Ramakrishnan, and G. Steinle, Semicond. Sci. Technol. **17**, 892 (2002).
[2] J. S. Harris, Jr., Semicond. Sci. Technol. **17**, 880 (2002).
[3] A. Mascarenhas and Yong Zhang, Curr. Opin. Solid State Mater. Sci. **5**, 253 (2001).
[4] J. F. Geisz and D. J. Friedman, Semicond. Sci. Technol. **17**, 769 (2002).
[5] I. A. Buyanova, W. M. Chen, G. Pozina, J. P. Bergman, B. Monemar, H. P. Xin, and C. W. Tu, Appl. Phys. Lett. **75**, 501 (1999).
[6] K. Matsuda, T. Saiki, M. Takahashi, A. Moto, and S. Takagishi, Appl. Phys. Lett. **78**, 1508 (2001).
[7] A. M. Mintairov, P. A. Blagnov, J. L. Merz, V. M. Ustinov, A. S. Vlasov, A. R. Kovsh, J. S. Wang, L. Wei, and J. Y. Chi, Physica E (Amsterdam) **21**, 385 (2004).
[8] J. L. Merz, A. M. Mintairov, T. Kosel, and K. Sun, IEE Proc.: Optoelectron. **151**, 346 (2004).
[9] C. Skierbiszewski *et al.*, Phys. Statatus Solidi B **216**, 135 (1999).
[10] D. Fowler, O. Makarovsky, A. Patanè, L. Eaves, L. Geelhaar, and H. Riechert, Phys. Rev. B **69**, 153305 (2004).
[11] A. J. Ptak, S. W. Johnson, S. Kurtz, D. J. Friedman, and W. K. Metzer, J. Cryst. Growth **251**, 392 (2003).
[12] D. L. Young, J. F. Geisz, and T. J. Coutts, Appl. Phys. Lett. **82**, 1236 (2003).
[13] R. Mouillet, L. A. de Vaulchier, E. Deleporte, Y. Guldner, L. Traves, and J. C. Harmand, Solid State Commun. **126**, 333 (2003).
[14] F. Masia *et al.*, Phys. Rev. B **73**, 073201 (2006).
[15] A. M. Mintairov, T. H. Kosel, J. L. Merz, P. A. Blagnov, A. S. Vlasov, V. M. Ustinov, and R. E. Cook, Phys. Rev. Lett. **87**, 277401 (2001).
[16] H. A. McKay, R. M. Feenstra, T. Schmidtling, and U. W. Pohl, Appl. Phys. Lett. **78**, 82 (2001).
[17] H. A. McKay, R. M. Feenstra, T. Schmidtling, U. W. Pohl, and J. F. Geisz, J. Vac. Sci. Technol. B **19**, 1644 (2001).
[18] A. Lindsay and E. P. O'Reilly, Phys. Rev. Lett. **93**, 196402 (2004).
[19] A. Lindsay and E. P. O'Reilly, Physica E (Amsterdam) **21**, 901 (2004).
[20] S. Fahy, A. Lindsay, H. Ouerdane, and E. P. O'Reilly, Phys. Rev. B **74**, 035203 (2006).
[21] J. Neugebauer and C. G. Van de Walle, Phys. Rev. B **51**, 10568 (1995).
[22] R. S. Goldman, R. M. Feenstra, B. G. Briner, M. L. O'Steen, and R. J. Haustein, Appl. Phys. Lett. **69**, 3698 (1996).
[23] A. M. Mintairov, P. A. Blagnov, V. G. Melehin, N. N. Faleev, J. L. Merz, Y. Qiu, S. A. Nikishin, and H. Temkin, Phys. Rev. B **56**, 15836 (1997).
[24] S. Francoeur, S. A. Nikishin, C. Jin, Y. Qiu, and H. Temkin, Appl. Phys. Lett. **75**, 1538 (1999).

[25] S. B. Zhang and Su-Huai Wei, Phys. Rev. Lett. **86**, 1789 (2001).
[26] I. S. Shlimak, A. L. Efros, and I. Ya. Yanchev, Sov. Phys. Semicond. **11**, 149 (1977).
[27] S. Fahy and E. P. O'Reilly, Appl. Phys. Lett. **83**, 3731 (2003).
[28] E. D. Jones, A. A. Allerman, S. R. Kurtz, N. A. Modine, K. K. Bajaj, S. T. Tozer, and X. Wei, Phys. Rev. B **62**, 7144 (2000).
[29] S. M. Lee and K. K. Bajaj, J. Appl. Phys. **73**, 1788 (1993).
[30] R. T. Senger and K. K. Bajaj, J. Appl. Phys. **94**, 7505 (2003).
[31] O. Rubel, M. Galluppi, S. D. Baranovskii, K. Volz, L. Geelhaar, H. Riechert, P. Thomas, and W. Stolz, J. Appl. Phys. **98**, 063518 (2005).
[32] S. D. Baranovskii, R. Eichmann, and P. Thomas, Phys. Rev. B **58**, 13081 (1998).
[33] F. Mandl, *Quantum Mechanics*, 2nd ed. (Butterworths, London, 1957).
[34] D. Monroe, Phys. Rev. Lett. **54**, 146 (1985).
[35] B. I. Halperin and M. Lax, Phys. Rev. **153**, 802 (1967).
[36] R. Zimmermann, F. Grosse, and E. Runge, Pure Appl. Chem. **69**, 1179 (1997).
[37] G. Martino, G. Pistone, S. Savasta, O. Di Stefano, and R. Girlanda, J. Phys.: Condens. Matter **18**, 2367 (2006).